AERODYNAMIC VALIDATION OF A SCAR DESIGN

Robert L. Roensch
McDonnell Douglas Corporation

SUMMARY

The results of a wind tunnel test of a model of the McDonnell Douglas Supersonic Cruise Aircraft justify the design procedures used to develop the configuration. The data obtained with a baseline and improved performance wing support the analysis and design methods. The minimum drag is almost exactly as predicted. Despite small discrepancies in the predicted level of drag-due-to-lift, the increments between configurations are as predicted and can be used to identify further improvements in performance. The results also verified the aerodynamic efficiency of the configuration with a demonstrated trimmed L/D_{max} of 9.1. It should be noted that this configuration was not optimized solely for aerodynamics, but was tailored to provide a good match between structural and aerodynamic performance.

There is demonstrable evidence that known refinements are possible to raise the L/D_{max} to 9.6, and a goal of 10.3 has been set for technology research as a realistic target for an arrow wing design at a Mach number of 2.2.

INTRODUCTION

A wind tunnel test* of the McDonnell Douglas Supersonic Cruise Aircraft, designed for a cruise Mach number of 2.2, was conducted in the NASA Ames Unitary Plan Wind Tunnels. Extensive force, pressure, and flow visualization data were obtained over a Mach number range from 0.5 to 2.4. Comparisons between theory and measurements of both forces and pressures presented in this paper concentrate on the results obtained in the 9-Foot by 7-Foot Supersonic tunnel. Schlieren and tuft pictures are presented to help provide an understanding of the nonlinearities observed at off-design conditions.

---

*This work was performed as an MDC-NASA cooperative program under NASA Contract NAS1-13633 and will be published as a contract report entitled "Aerodynamic Characteristics of a Mach 2.2 Advanced Supersonic Cruise Aircraft Configuration at Mach Numbers from 0.5 to 2.4."

SYMBOLS

Values are given in both SI and U.S. Customary Units. The measurements and calculations were made in U.S. Customary Units.

α	angle of attack, deg.
B_1	fuselage
C_D	drag coefficient
C_L	lift coefficient
C_m	pitching moment coefficient about 1/4 MAC
C_{n_β}	variation of yawing moment coefficient with sideslip angle, 1/rad (1/deg.)
CG,cg	center of gravity
C_P	pressure coefficient
ΔC_D	increment in drag coefficient
L/D_{max}	maximum lift-to-drag ratio
M	Mach number
MAC	mean aerodynamic chord of the trapezoidal wing formed by extending the leading and trailing edges of the outer panel to the aircraft centerline
Y/(b/2)	spanwise location in fraction of semi-span
W_1,W_2,W_3	wings
N_1,N_2	nacelles

CONFIGURATION

A three view of the MDC Supersonic Cruise Aircraft is shown in figure 1. This 273-passenger aircraft is designed for ranges in excess of 8300 km (4500 n.mi) at a takeoff gross weight of 340,194 kg (750,000 lb). It features a 929 m^2 (10,000 ft^2) arrow-type wing designed for a cruise Mach number of 2.2 with the planform based on the NASA SCAT-15F concept, a conventional horizontal tail, a single fuselage-mounted vertical tail, and four engines mounted in axisymmetric nacelles. The inboard leading edge of the wing has a sweep of 71 degrees with the sweep reduced to 57 degrees outboard of the leading edge break. The average thickness ratio of the wing is slightly less than three percent. The thickness ratio is equal to 2.25 percent of the chord at the wing root and

is constant at three percent of the chord from the trailing edge break to the wing tip. The development of this configuration has been described in some detail in references 1, 2, and 3.

WIND TUNNEL TEST

A cooperative MDC-NASA wind tunnel test program using a 1.5-percent scale model of this configuration was conducted in the NASA Ames Unitary Plan Wind Tunnels in the latter part of 1975. Data were obtained at Mach numbers from 0.5 to 1.3 in the 11-Foot Transonic tunnel and at Mach numbers from 1.6 to 2.4 in the 9-Foot x 7-Foot Supersonic tunnel. All the data were obtained at a Reynolds number of slightly less than four million based on the model MAC. The aft portion of the fuselage of the model departed somewhat from the aircraft in order to accommodate the balance and sting as can be seen in the photographs of the model installed in the Supersonic tunnel (fig. 2) and the Transonic tunnel (fig. 3). Extensive pressure data were obtained along with the force data, as well as tuft and schlieren flow visualization photographs.

Three different wings were tested during the program along with two different nacelle inlet designs. The following pertinent model designations were used for the test:

B_1	baseline model fuselage.
W_1	wing optimized at a C_L of 0.1 without regard to trim drag.
W_2	improved performance wing optimized at a C_L of 0.1 with a pitching moment constraint to reduce the trim drag.
W_3	wing W_1 with a fairly sophisticated reflex in the region of the nacelles to relieve the nose down pitching moments generated by the nacelle flow field.
N_1	external compression inlet with a cowl lip angle of 24 degrees.
N_2	mixed compression inlet with a cowl lip angle of 6 degrees.

The results of the nacelle and wing reflex test are presented fairly completely in reference 4 and are only summarized here. The wing reflex tested was not totally successful since it cancelled only about 75 percent of the nacelle induced pitching moment. A simpler reflex concept may well be adequate for this task. Further wind tunnel tests are necessary to develop the optimum geometry. The wave drag with the external compression inlet was approximately five drag counts ($\Delta C_D = 0.0005$) higher than with the mixed compression inlet. This is the magnitude of the difference predicted by the method of characteristics analysis (ref. 5).

TEST RESULTS

The majority of the presentation deals with the results obtained with wing W_2. Comparisons of the wind tunnel data for the wing-body configuration with theory are shown in figures 4, 5, and 6. The wind tunnel data have been corrected to full scale aircraft conditions. In addition to the skin friction correction for the difference between flight Reynolds number and the wind tunnel test Reynolds number, the measured drag has been increased to account for the estimated difference between the wave drag of the open afterbody of the model and the closed aft fuselage of the aircraft. The drag-due-to-lift, the lift, and the pitching moment have also been corrected for the estimated difference in each of these parameters due to the afterbody shapes of the model and the aircraft.

The zero-lift wave drag of the configuration was estimated using the MDC-developed Arbitrary Body Wave Drag program (ref. 6) which calculates, based on the area rule theory (ref. 7 and 8), the wave drag of completely arbitrary configurations. All analyses were performed with the full geometry of the configuration at the cruise attitude. Drag-due-to-lift, lift, and wing-body pitching moments were calculated with the MDC version of the Woodward program (ref. 9) by a direct analysis of the wing-body configuration including wing thickness and body camber effects. Since the Woodward program, when run with wing and body thickness, includes a zero-lift wave drag, an uncambered version of the configuration was analyzed with the Woodward program to obtain a Woodward wave drag. This was subtracted from the cambered configuration Woodward drag analysis and the remainder is considered to be the drag-due-to-lift including the twist drag.

As can be seen by the drag polars shown in figure 4, the agreement between the estimated and measured minimum drag of the configuration across the Mach number spectrum is excellent. The calculated drag-due-to-lift, however, shows a trend of overprediction at the lower supersonic Mach numbers and underprediction at the higher Mach numbers. Almost perfect agreement is obtained at Mach 2.0, 0.2 below the design Mach number. This would suggest that perhaps the configuration should be designed for a Mach number 0.2 higher than the desired cruise Mach number. Earlier NASA SCAT wind tunnel tests found a similar phenomenon to exist.

The agreement of the data with the calculated lift curves shown in figure 5 is reasonably good, though there is a slight overprediction of the lift which increases as the Mach number increases.

The pitching moment characteristics shown in figure 6 show fairly good agreement between the data and the estimate near the cruise C_L, which is approximately 0.11. At the Mach 2.2 design condition the measured aerodynamic center is approximately 2.5 percent of MAC ahead of the estimated value. At higher C_L's the data show evidence of a mild pitchup. The magnitude is not considered to be a significant problem because the horizontal tail has sufficient control authority to compensate for this deviation from linear pitching moments using only a fraction of the available tail effectiveness, even at the design load

factor. The tail-on data show the same trends, with the horizontal tail effectiveness relatively insensitive to angle of attack.

The pressure data obtained during this test help explain the nonlinear behavior of the pitching moments. Shown in figure 7 are the estimated and measured pressures at Mach 2.2 on the upper and lower surface of the wing at an angle of attack of 2.5 degrees, which is near the cruise angle of attack. The agreement between the Woodward program predictions and the data is fairly good. However, there is a lack of agreement at high angles of attack as shown in figure 8, which is not unexpected. The linear theory pressure coefficients are predicted to exceed the vacuum limited C_p which is approximately equal to $1/M^2$ (about -0.2 at Mach 2.2) over much of the upper surface of the wing, particularly on the outer wing panel. The measured lower surface pressures are in reasonably good agreement with the linear theory on the inboard portion of the wing, but there is a significant deviation on the outer panel. These two effects, limiting C_p's on the upper surface and less than predicted positive pressures on the lower surface, contribute to a loss in outer panel loading at high angles of attack which results in the mild pitchup observed.

Small mini-tufts were attached to the wing to learn how the flow field varies as the upper surface reaches the limiting C_p. The results are shown in figure 9. At the lower angle of attack the flow is very well behaved. At the high angle of attack, it can be seen that the flow has changed character considerably but there is no evidence of any flow separation. The tufts on the lower surface showed no significant variation over this range of angle of attack. Schlieren photographs taken from the top of the model over the same angle of attack range show that the shock wave which is created at the leading edge break sweeps forward as the angle of attack is increased (fig. 10).

The pressure, flow visualization, and force data obtained during this test clearly identify the cause of the nonlinear behavior of the pitching moments. The arrow-wing concept is characterized by fairly high loading of the outer panel which will cause the upper surface to reach limiting C_p's at moderate C_L's. While this does result in a mild pitchup, there are some favorable side benefits in the structural area. The structural loads that the outer panel must carry at supersonic speeds do not grow as rapidly with load factor as the linear theory would predict. This may result in a reduction in the wing weight from that estimated using linear theory loads.

Yawed polars and a limited number of constant angle of attack yaw sweeps were obtained to evaluate the lateral-directional characteristics of the configuration. Of interest was whether a single fuselage mounted vertical tail would provide adequate directional stability throughout the flight envelope of the aircraft. This can be particularly significant at low speeds and high angles of attack.

The tail-on and tail-off directional stability characteristics (C_{n_β}) of the model are shown in figure 11. In the subsonic range, no significant deterioration of the vertical tail effectiveness occurred within the angle of attack range for which data were obtained. It is anticipated that the tail effectiveness will be reduced at higher angles of attack. This will require

the use of strakes on the nose similar to those used on the Concorde and the DC-9-50 to provide satisfactory directional stability characteristics at high sideslip angles at high angles of attack in the low speed flight regime. The supersonic data show that from Mach 1.6 to 2.4 there is a gradual degradation in vertical tail effectiveness as the angle of attack is increased. But, at conditions corresponding to the design load factor ($C_L \cong 0.27$) the configuration shows positive directional stability.

VALIDATION OF DESIGN PROCEDURES

The extent to which the wind tunnel test provides validation of the design procedures used for developing this configuration is shown by comparing the wing-body characteristics of the baseline wing and the improved performance wing at Mach 2.2. As shown in figure 12, the incremental differences in all the coefficients are nearly as predicted. The change in the pitching moment observed between W_1 and W_2 is of special interest because the design of W_2 was predicated on making the wing-body pitching moments positive, requiring an up-tail load to trim the aircraft.

The value of this concept is shown in figure 13. The trimmed L/D_{max} shown as a function of cg location includes the skin friction and wave drag of the horizontal and vertical tails as well as the trim drag due to the horizontal tail lift and drag-due-to-lift. While the level of experimental L/D_{max} is slightly less than predicted, the experimental increments between W_1 and W_2 are almost as predicted. This figure also points out the real benefit obtained by optimizing the wing for a desired pitching moment. The highest achievable L/D_{max} can be obtained within desired cg limits. The cg limits shown were chosen so that the aft supersonic limit corresponds to the subsonic neutral point, an MDC design requirement for this configuration.

CONCLUSIONS

The results of a wind tunnel test of a model of the McDonnell Douglas Supersonic Cruise Aircraft justify the design procedures used to develop the configuration. The data obtained with a baseline and improved performance wing support the analysis and design methods, with the possible exception of some discrepancy in the prediction of the drag-due-to-lift. However, even with discrepancies in the predicted level of drag-due-to-lift, the increments between configurations are as predicted and can be used to identify further improvements in performance. The results also verified the good aerodynamic efficiency of the configuration with a demonstrated trimmed L/D_{max} of 9.1. It should be noted that this configuration was not optimized solely for aerodynamics, but was tailored to provide a good match between structural and aerodynamic performance.

There is demonstrable evidence that known refinements are possible to raise the L/D_{max} to 9.6, and a goal of 10.3 has been set for technology

research as a realistic target for an arrow wing design at a Mach number of 2.2.

The value of obtaining wing pressure distributions as well as force and flow visualization data, even during the early stages of the development of a configuration, was amply demonstrated. With this degree of detailed data it is possible to determine the true limitations of the linear theory used in the aircraft design process.

REFERENCES

1. FitzSimmons, R. D. and Hoover, W. C.: AST-A Fifth Engine for Environmental Consideration. SAE Paper 730899, 1973.

2. FitzSimmons, R. D. and Roensch, R. L.: Advanced Supersonic Transport. SAE Paper 750617, 1975.

3. Radkey, R. L., Welge, H. R., and Roensch, R. L.: Aerodynamic Design of a Mach 2.2 Supersonic Cruise Aircraft. AIAA Paper No. 76-955, 1976.

4. Welge, H. R., Radkey, R. L., and Henne, P. A.: Nacelle Aerodynamic Design and Integration on a Mach 2.2 Supersonic Cruise Aircraft. AIAA Paper No. 76-757, 1976.

5. Henne, P. A.: Unique Application of the Method of Characteristics to Inlet and Nozzle Design Problems. AIAA Paper No. 75-1185, 1975.

6. Gentry, A. E., Smyth, D. N., and Oliver, W. R.: The Mark IV Supersonic-Hypersonic Arbitrary-Body Program. AFFDL-TR-73-159, 1973.

7. Jones, R. T.: Theory of Wing-Body Drag at Supersonic Speeds. NACA Report 1284, 1956. (Supersedes NACA RM A53H18a, 1953.)

8. Whitcomb, R. T.: A Study of the Zero-Lift Drag Rise Characteristics of Wing-Body Combinations Near the Speed of Sound. NACA Report 1273, 1956. (Supersedes NACA RM L52H08, 1952.)

9. Woodward, F. A., Tinoco, E. N., and Larson, J. W.: Analysis and Design of Supersonic Wing-Body Combinations, Including Flow Properties in the Near Field. NASA CR-73106, 1967.

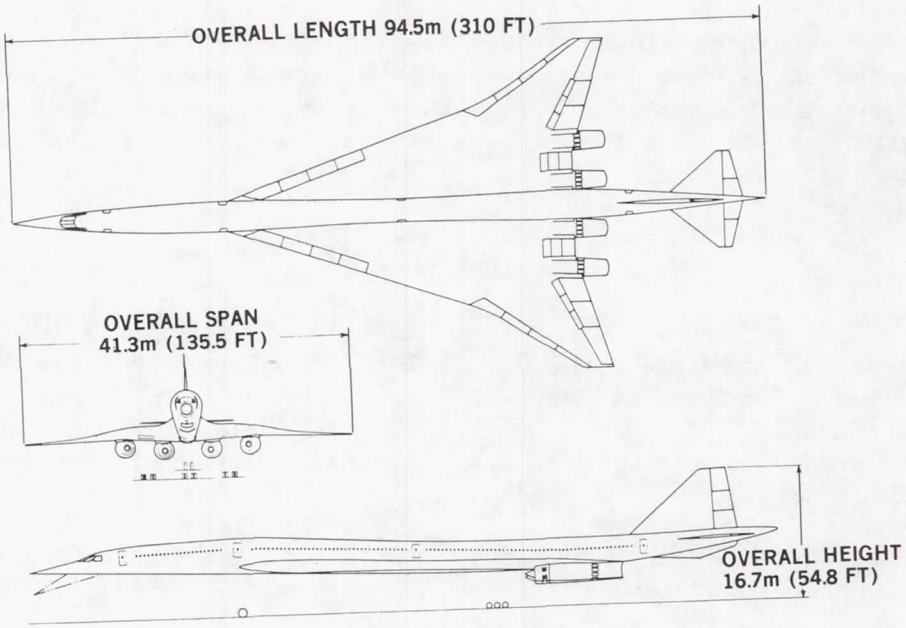

Figure 1.- MDC baseline supersonic cruise aircraft.

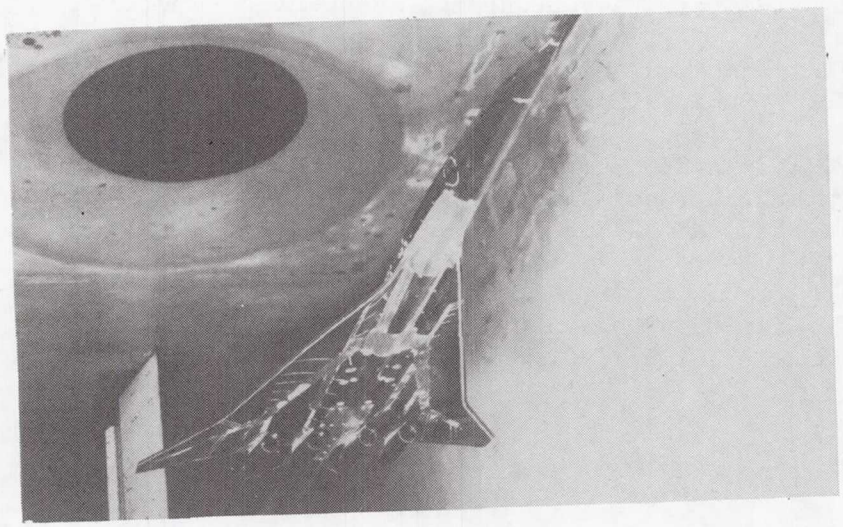

Figure 2.- Model in Ames 9-foot by 7-foot tunnel.

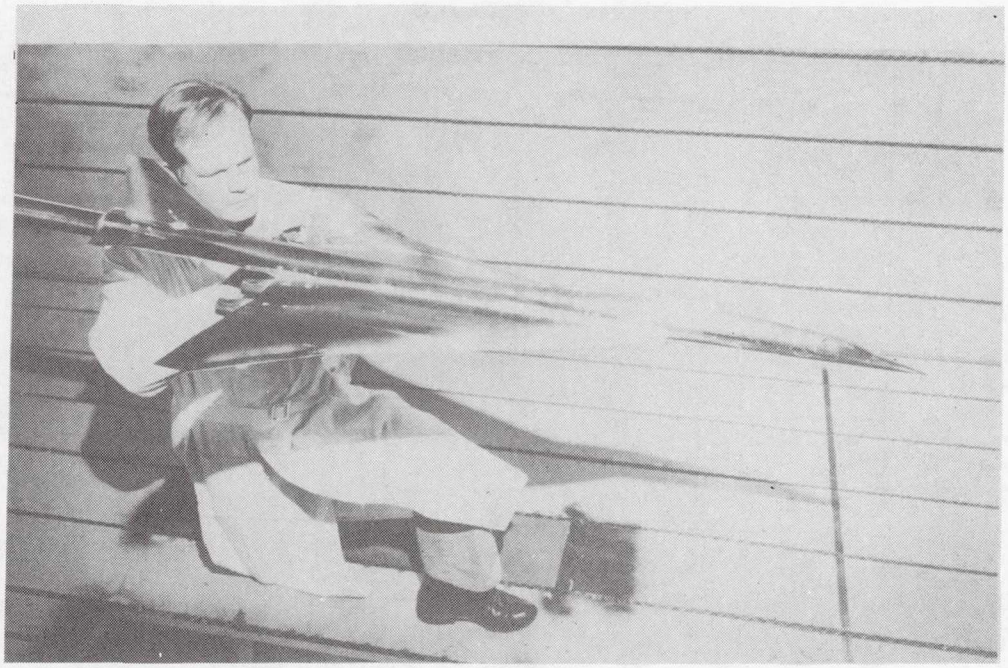

Figure 3.- Model in Ames 11-foot tunnel.

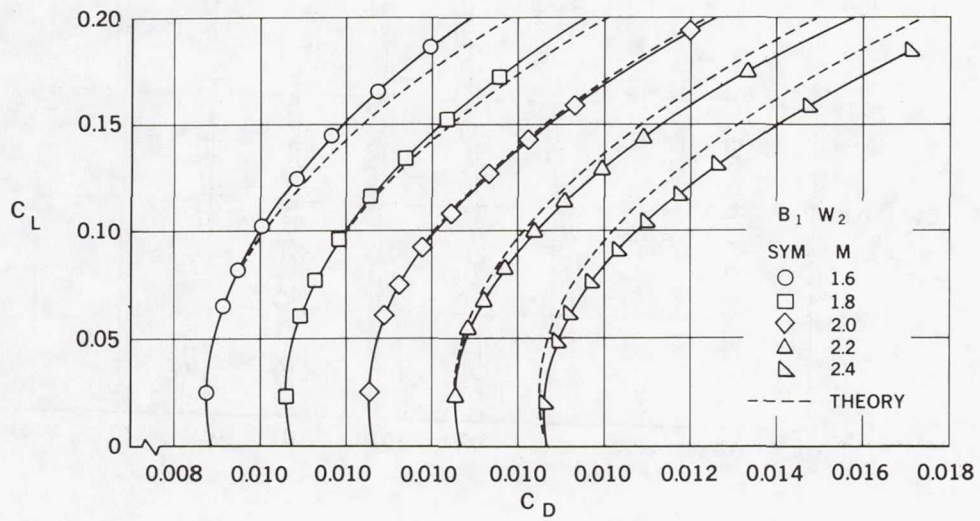

Figure 4.- Wing-body drag polars.

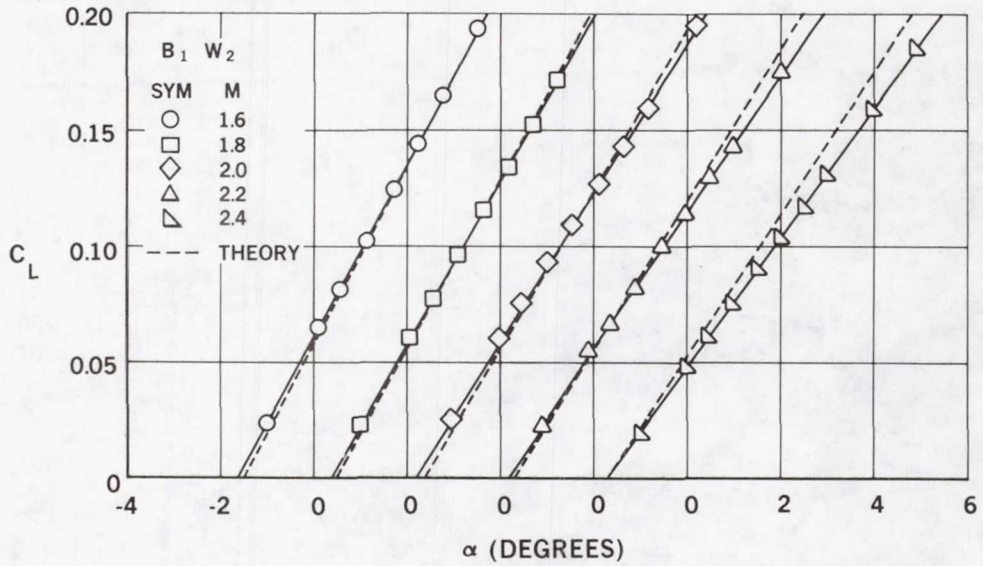

Figure 5.- Wing-body lift curves.

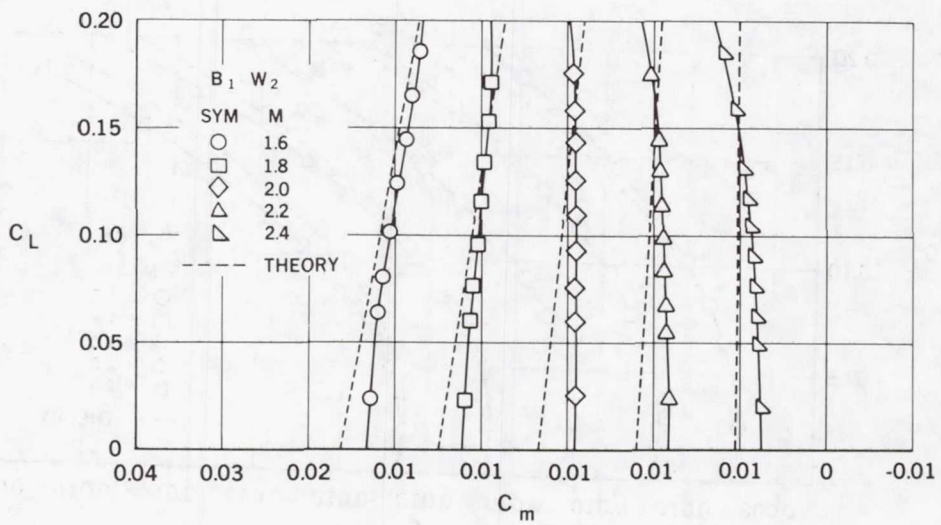

Figure 6.- Tail-off pitching moment characteristics.

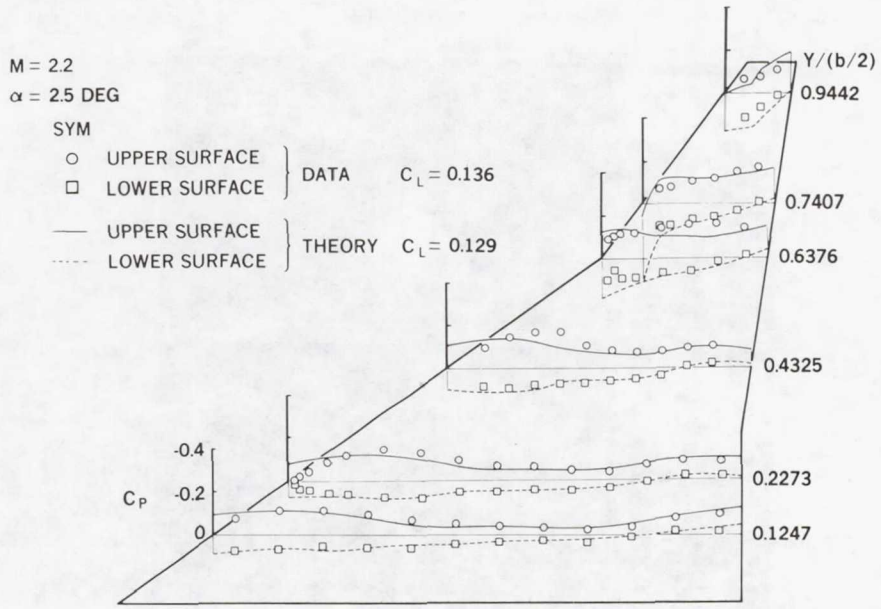

Figure 7.- Low angle of attack calculated and experimental pressure distributions on B_1W_2.

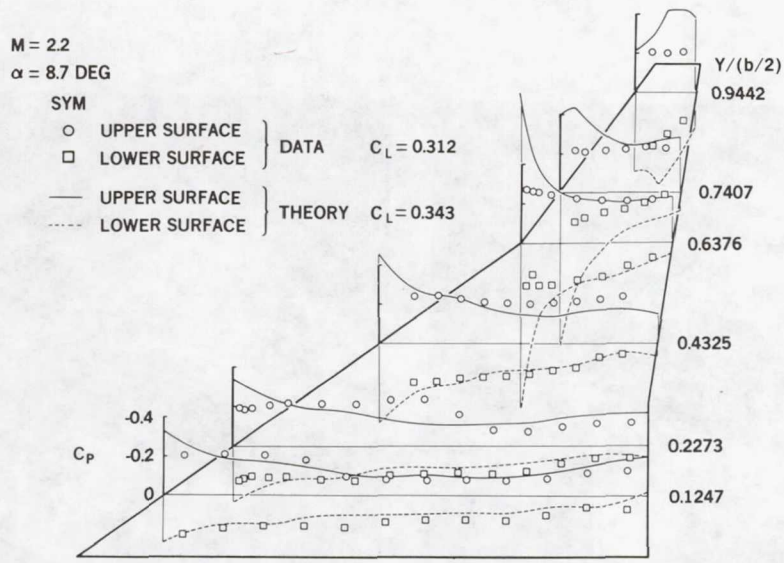

Figure 8.- High angle of attack calculated and experimental pressure distributions on B_1W_2.

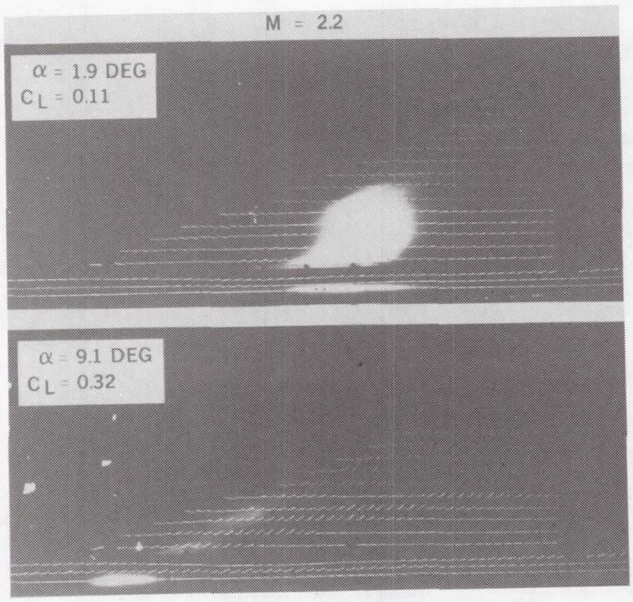

Figure 9.- Upper surface tufts.

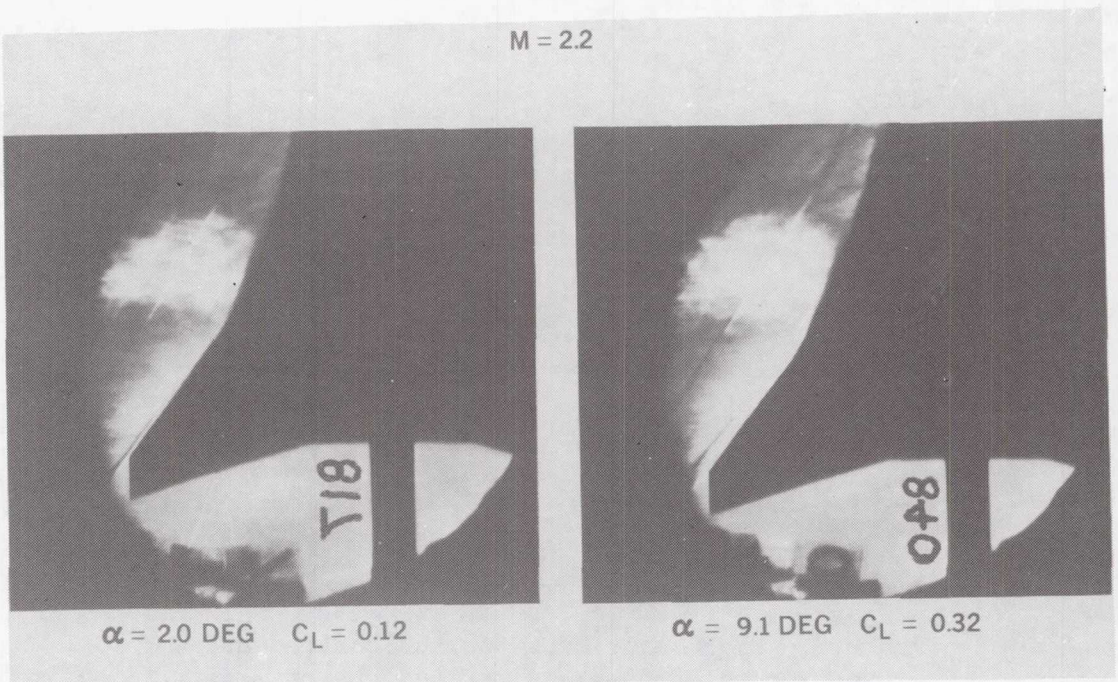

Figure 10.- Schlieren photographs.

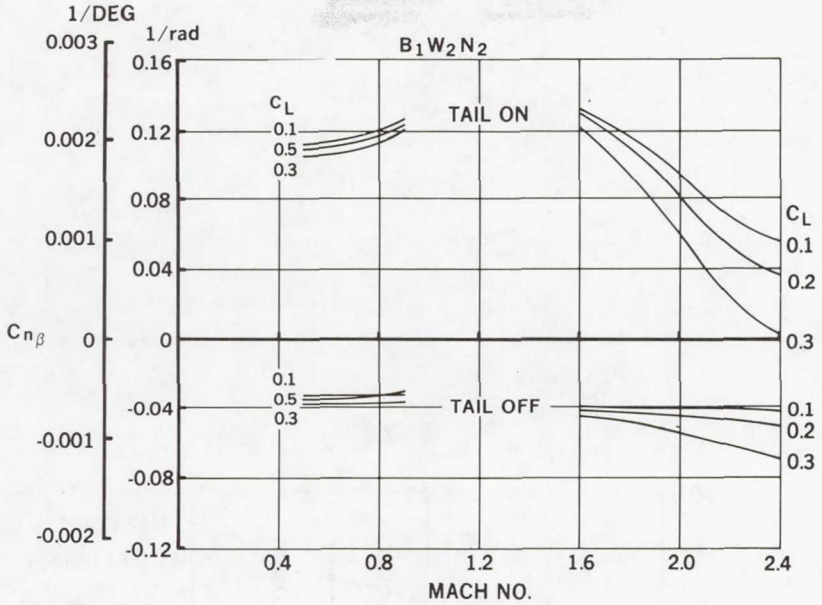

Figure 11.- Measured directional stability characteristics.

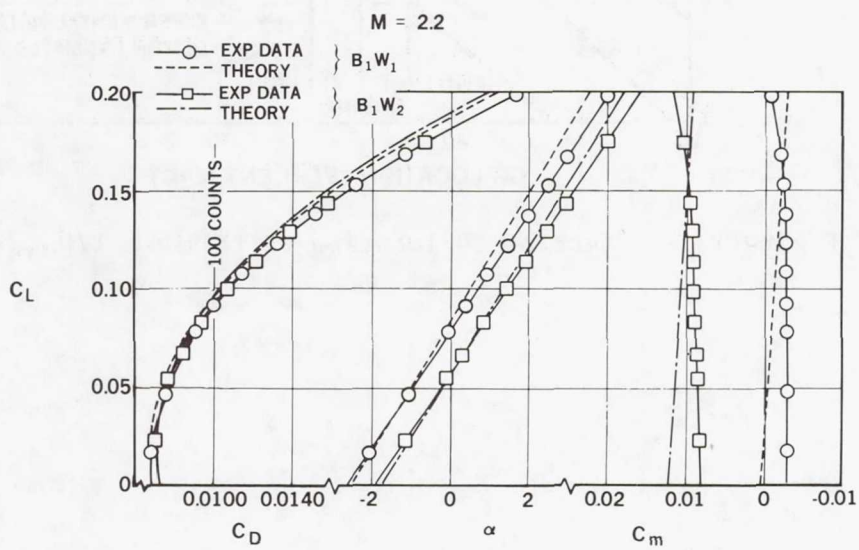

Figure 12.- Comparison of wing-body characteristics for two wing designs.

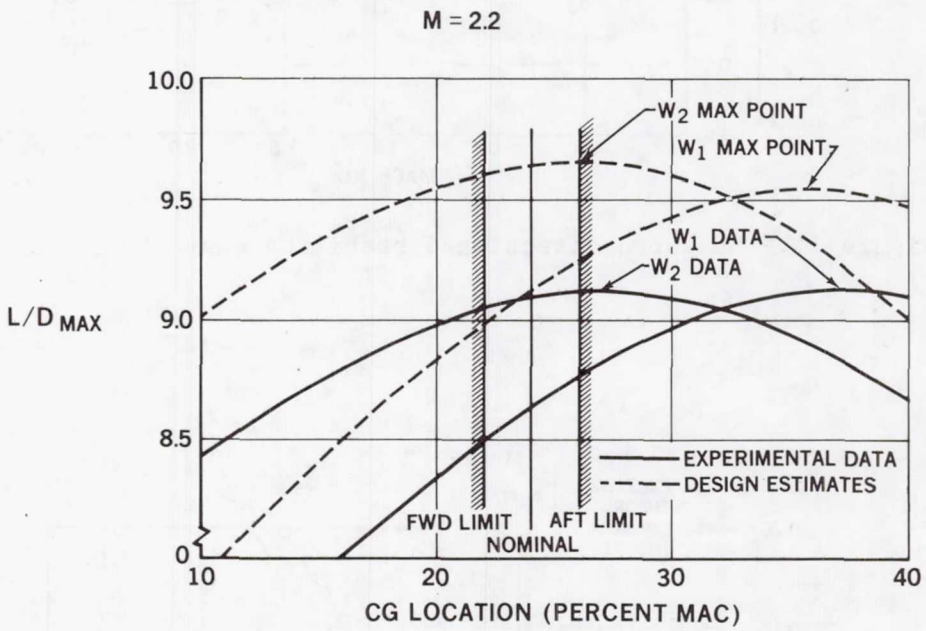

Figure 13.- Effect of CG location on trimmed L/D_{max}.

SESSION II - STABILITY AND CONTROL